

Magic wavelength of the $^{138}\text{Ba}^+$ $6s\ 2S_{1/2} - 5d\ 2D_{5/2}$ clock transition

S. R. Chanu,¹ V. P. W. Koh,² K. J. Arnold,¹ R. Kaewuam,¹ T. R. Tan,^{1,2} Zhiqiang Zhang,¹ M. S. Safronova,^{3,4} and M. D. Barrett^{1,2,*}

¹Centre for Quantum Technologies, National University of Singapore, 3 Science Drive 2, 117543 Singapore

²Department of Physics, National University of Singapore, 2 Science Drive 3, 117551 Singapore

³Department of Physics and Astronomy, University of Delaware, Newark, Delaware 19716, USA

⁴Joint Quantum Institute, National Institute of Standards and Technology
and the University of Maryland, College Park, Maryland, 20742

The zero crossing of the dynamic differential scalar polarizability of the $S_{1/2} - D_{5/2}$ clock transition in $^{138}\text{Ba}^+$ has been determined to be 459.1614(28) THz. Together with previously determined matrix elements and branching ratios, this tightly constrains the dynamic differential scalar polarizability of the clock transition over a large wavelength range ($\gtrsim 700$ nm). In particular it allows an estimate of the blackbody radiation shift of the clock transition at room temperature.

PACS numbers: 06.30.Ft, 06.20.fb

Singly-ionized barium has been well studied over the years with a wide range of precision measurements [1–8] that have provided valuable benchmark comparisons for theory [9–14]. It was recently proposed that some of these measurements, specifically high accuracy measurements of transition matrix elements and branching ratios, could be used to construct an accurate representation of the dynamic differential scalar polarizability, $\Delta\alpha_0(\omega)$ of the $S_{1/2} - D_{5/2}$ clock transition over a large wavelength range [15]. Crucial to that proposal was a determination of a zero crossing $\Delta\alpha_0(\omega_0) = 0$ near 653 nm, which bounds significant contributions to $\Delta\alpha_0(\omega)$ from the ultraviolet (uv) spectrum. Here we determine ω_0 with an inaccuracy of a few GHz.

To find ω_0 , a linearly polarized laser beam near 653 nm is focussed onto the ion to induce an ac Stark shift of the clock transition and the shift measured as a function of the laser frequency ω . The ac Stark shift, $\delta_s(M_J)$, induced by the 653-nm laser is given by

$$\delta_s(M_J) = -\frac{1}{2}\Delta\alpha_0(\omega)\langle E^2 \rangle - \frac{1}{4}\alpha_2(\omega)\frac{3M_J^2 - J(J+1)}{J(2J-1)}(3\cos^2\theta - 1)\langle E^2 \rangle, \quad (1)$$

where M_J denotes the applicable eigenstate of $D_{5/2}$, $\alpha_2(\omega)$ is the dynamic tensor polarizability of $D_{5/2}$, and θ is angle between the 653-nm laser polarization and the quantization axis. The tensor component can be eliminated by determining the average ac Stark shift

$$\delta_0(\omega) = \frac{1}{3}[\delta_s(1/2) + \delta_s(3/2) + \delta_s(5/2)] \quad (2)$$

$$= -\frac{1}{2}\Delta\alpha_0(\omega)\langle E^2 \rangle \quad (3)$$

Hence, with the laser intensity fixed, $\delta_0(\omega)$ is directly proportional to $\Delta\alpha_0(\omega)$, which is approximately linear

in a neighbourhood of ω_0 . Consequently, ω_0 can be determined from a linear fit to measurements of $\delta_0(\omega)$ as a function of ω with an accuracy limited by the projection noise of the measurements, and a small nonlinearity in $\Delta\alpha_0(\omega)$, which can be estimated from theory.

Although the laser power is actively stabilized outside the experiment chamber, etaloning effects and uncalibrated frequency response of the detector can give rise to a frequency dependence of the resulting laser intensity at the ion. In addition, pointing stability of the laser can also degrade the accuracy of the ac Stark shift measured at a single frequency. To compensate these effects, one can make use of the weighted average

$$\delta_2(\omega) = \frac{25}{42}\left(\delta_s(5/2) - \frac{1}{5}\delta_s(3/2) - \frac{4}{5}\delta_s(1/2)\right) \quad (4)$$

$$= -\frac{1}{4}\alpha_2(\omega)(3\cos^2\theta - 1)\langle E^2 \rangle \quad (5)$$

which is a measure of the tensor polarizability. The ratio $\delta_0(\omega)/\delta_2(\omega)$ is then independent of slow variations in the intensity but has the same zero crossing. In addition, setting $\theta \approx \pi/2$ minimizes the influence of magnetic field pointing stability, which would compromise the stability of $\delta_2(\omega)$.

Measurements are carried out in a linear Paul trap with axial end-caps, the details of which have been given elsewhere [16, 17]. The rf potential at a frequency near $\Omega_{\text{rf}} = 2\pi \times 20.7$ MHz is delivered via a quarter-wave helical resonator. Together with static end-cap and bias potentials, the measured trap frequencies of a single $^{138}\text{Ba}^+$ are $\sim (810, 925, 245)$ kHz, with the lowest frequency along the trap axis.

The relevant level structure of $^{138}\text{Ba}^+$ is illustrated in Fig. 1(a). Doppler cooling is provided by driving the 493- and 650-nm transitions, with light scattered at 650 nm collected onto a single photon counting module (SPCM) for detection. The $D_{5/2}$ level is populated by driving the $S_{1/2} - D_{5/2}$ clock transition at 1762 nm and depopulated by driving the $D_{5/2} - P_{3/2}$ transition at 614 nm. State preparation into the $m = \pm 1/2$ states of the $S_{1/2}$ levels

* phybmd@nus.edu.sg

is facilitated by two additional 493-nm beams that are σ^\pm polarized.

Laser configurations are illustrated in Fig. 1(b) and (c). Cooling and repumping light at 493, 614, and 650 nm are all collinear and propagate at 45 degrees to the $\hat{\mathbf{z}}$ -axis. All three beams are linearly polarized with the 650-nm and 614-nm lasers polarized orthogonal to the 493-nm laser, which is polarized along the imaging axis ($\hat{\mathbf{x}}$). The magnetic field lies in the horizontal (xz) plane at an angle of approximately 33 degrees to the $\hat{\mathbf{x}}$ -axis with a magnitude of ~ 0.2 mT, which is sufficient to lift the Zeeman degeneracy and prevent dark states when driving the $D_{3/2} - P_{1/2}$ and $D_{5/2} - P_{3/2}$ transitions. The clock laser at 1762 nm propagates almost co-linear with the imaging axis and is linearly polarized in the horizontal plane, which permits efficient coupling to the $|S_{1/2}, \pm 1/2\rangle$ to $|D_{5/2}, \pm M_J\rangle$ transitions for $M_J = 1/2, 3/2$, and $5/2$. A Stark-shifting laser near 653 nm propagates along $\hat{\mathbf{y}}$ and is linearly polarized orthogonal to the magnetic field. All lasers are switched by acousto-optic modulators (AOMs).

The 653-nm laser is provided by a tunable extended-cavity-diode laser (ECDL) together with an injection locked slave to boost the power. The laser is locked to a wavemeter with 10 MHz accuracy (High finesse WS8-10), which is routinely calibrated to a caesium-locked 852-nm diode laser. Control of the radio frequency (rf) power driving a switching AOM is used to stabilize the beam power, which is sampled by a beam pick-off before the vacuum chamber.

The 1762-nm clock laser is an ECDL, which is phase locked to an optical frequency comb (OFC). The short term (< 10 s) stability of the OFC is derived from a ~ 1 Hz linewidth laser at 848 nm which is referenced to a 10 cm long ultra-low expansion (ULE) cavity with finesse of $\sim 4 \times 10^5$. For longer times ($\gtrsim 10$ s), the OFC is steered to an active hydrogen maser (HM) reference. The 1762-nm laser is switched with an AOM, but frequency shifting is achieved via a wideband electro-optic modulator (EOM) with the lower sideband driving the transition of interest. Control of the rf power driving the EOM enables equal π -times for each clock transition.

A typical experiment consists of four steps: 1 ms of Doppler cooling, optical pumping for $50 \mu\text{s}$ to either $|S_{1/2}, m = \pm 1/2\rangle \equiv |S, \pm\rangle$, clock interrogation (Rabi) to $|D_{5/2}, \pm M_J\rangle$ for 1 ms, and finally detection for 1 ms. The initial Doppler cooling step includes the 614-nm beam to facilitate repumping from the upper clock state. When including the 653-nm beam to Stark shift the transition, the beam is switched on $200 \mu\text{s}$ before the clock laser, to ensure the beam power has stabilized.

The clock transition is realized by steering the clock laser to the average of the Zeeman pair $|S_{1/2}, \pm 1/2\rangle \leftrightarrow |D_{5/2}, \pm |M_J|\rangle$ to cancel linear Zeeman shifts of both levels. Using an interleaved servo in which the optical transition is alternately interrogated both with and without the 653-nm laser, the shift is determined from the difference frequency in the two configurations. In a single clock cycle, all three Zeeman pairs are measured: each

of the six transitions $|S_{1/2}, \pm 1/2\rangle - |D_{5/2}, \pm M_J\rangle$ for $M_J = 1/2, 3/2$, and $5/2$ is interrogated both sides of each transition, both with and without the 653-nm Stark shift beam. All 24 measurements are repeated $N = 50$ times. From these measurements error signals are derived to track the center and splitting for each Zeeman pair $|S_{1/2}, \pm 1/2\rangle - |D_{5/2}, \pm M_J\rangle$, both with and without the Stark shift. The ratio $\delta_0(\omega)/\delta_2(\omega)$ is inferred at each step from the appropriate frequency differences. The servo is first run for several clock cycles, to ensure each shifted and unshifted Zeeman pair is being tracked, and $\delta_0(\omega)/\delta_2(\omega)$ is inferred from a further 1000 cycles.

Measurements of $\delta_0(\omega)/\delta_2(\omega)$ were made over a frequency range of approximately ± 1 THz and are plotted in Fig. 2. Measurements at $\Delta f \approx -0.2, -0.6$ THz were measured 3 times giving 16 measurements in total. The fit is a linear regression using the projection noise expected from the 1000 measurements as uncertainties. The fit has $\chi^2_\nu = 1.15$ and an estimated zero crossing of $\Delta f = 59.2(1.8)$ GHz. However this does not account for bias arising from a linear fit to $\delta_0(\omega)/\delta_2(\omega)$.

To estimate the bias, we use theory to calculate $\delta_0(\omega)/\delta_2(\omega)$ at the frequencies used in the measurements, fit the resulting points to a straight line, and compare the interpolated zero crossing to that calculated from theory. This procedure indicates that a straight line fit would underestimate the zero crossing by ≈ 2.2 GHz. This does not change significantly if one offsets the frequencies used in the calculation by the small difference between the experimentally measured and calculated zero crossing. Consequently we apply 2.2 GHz as a correction, but we add, in quadrature, the full size of the correction to the uncertainty to obtain the final value of $\omega_0 = 2\pi \times 459.1614(28)$ THz. Note that, near to ω_0 , the 614 nm transition has a significant contribution to the curvature of both $\Delta\alpha_0(\omega)$ and $\alpha_2(\omega)$, but these contributions tend to cancel in the ratio. This explains the excellent linearity in Fig. 2 and the correspondingly small bias correction.

The measured ω_0 is in excellent agreement with the theoretical value of 459.10(92) THz given in [15]. The theory used more accurate, experimentally determined values of $\langle 6P_{1/2} \| r \| 6S_{1/2} \rangle$ and $\langle 6P_{3/2} \| r \| 6S_{1/2} \rangle$ from [4], but $\langle 6P_{3/2} \| r \| 5D_{5/2} \rangle$ and all uv contributions were determined from atomic structure calculations. The theoretical calculation gives $\Delta\alpha_0(\omega_0) \approx 0.5$ a.u., where a.u. denotes atomic units. The corresponding difference between theory and experiment could be readily explained by, for example, a change of 0.1% in $\langle 6P_{3/2} \| r \| 5D_{5/2} \rangle$ or 2% in $\langle 4F_{7/2} \| r \| 5D_{5/2} \rangle$; both of which are well within the suggested uncertainty of theory.

In [18], the value of $\langle 6P_{3/2} \| r \| 5D_{5/2} \rangle = 4.0911(31)$ a.u. was estimated using: measured branching ratios for $6P_{1/2}$ decays, the experimental value of $\langle 6P_{1/2} \| r \| 6S_{1/2} \rangle$ reported in [4], and a theoretically determined ratio $\langle 6P_{3/2} \| r \| 5D_{5/2} \rangle / \langle 6P_{1/2} \| r \| 5D_{3/2} \rangle$, with the latter expected to have high accuracy as it depends only weakly on correlation corrections. Using this value, together

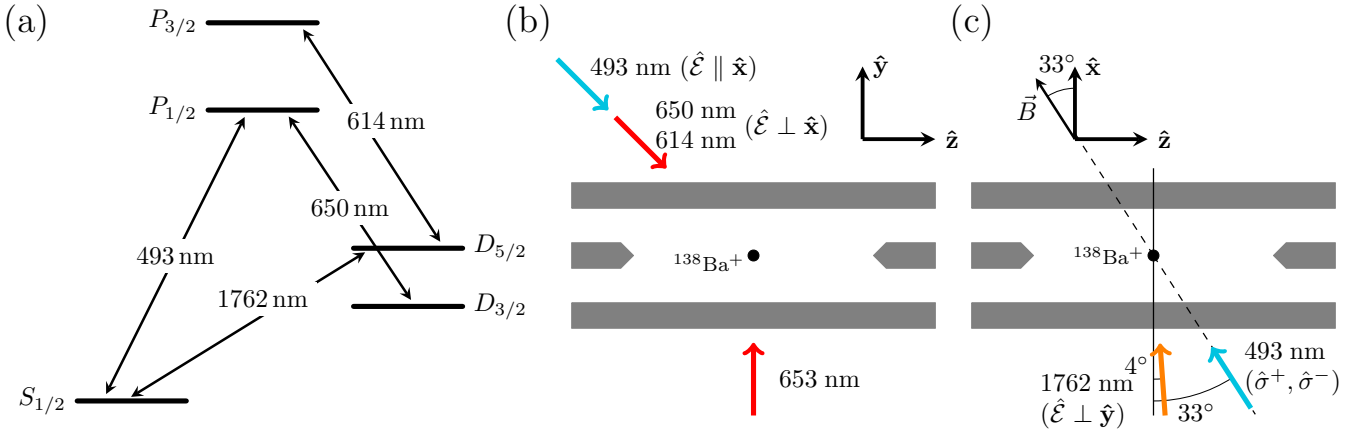


FIG. 1. (a) Level structure showing the Doppler cooling and detection transitions at 493 and 650 nm, the clock transition at 1762 nm, and the repumping transition at 614 nm. (b) and (c) Laser configurations used in the experiment. The σ^+ (σ^-) beams at 493 nm facilitate optical pumping into $|S_{1/2}, +1/2\rangle$ ($|S_{1/2}, -1/2\rangle$). The 653-nm is used to induce an ac Stark shift and is linearly polarized orthogonal to the magnetic field. Orientation and polarization of the 1762-nm clock laser permits efficient coupling to the $|S_{1/2}, \pm 1/2\rangle$ to $|D_{5/2}, \pm M_J\rangle$ transitions for $M_J = 1/2, 3/2$, and $5/2$.

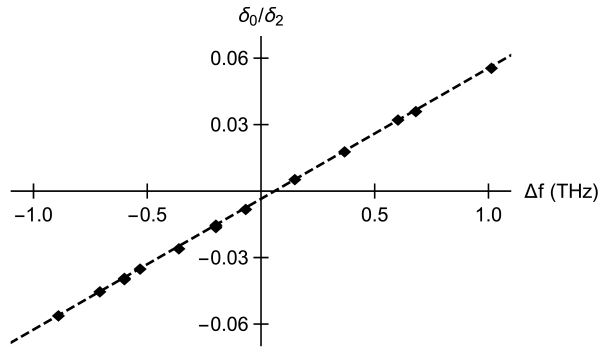


FIG. 2. Ratio of scalar to tensor shifts as a function of frequency difference relative to 459.1 THz. Error bars are smaller than the points and have been omitted. Measurements at $\Delta f \approx -0.2, -0.6$ THz were measured 3 times giving 16 measurements in total. Dashed line is from a χ^2 -fit.

with theoretical estimates of the uv terms in [15], gives a calculated value of $\Delta\alpha_0(\omega_0) \approx -0.77$ a.u., again consistent with reasonable variations of the uv contributions.

If we further apply the formalism in [15] using the same estimate for $\langle 6P_{3/2} | r | 5D_{5/2} \rangle$, we may approximate $\Delta\alpha_0(\omega)$ by

$$\Delta\alpha_0(\omega) = \Delta\alpha_0^{\text{vis}}(\omega) - \frac{\Delta\alpha_0^{\text{vis}}(\omega_0) [1 - (\omega_0/\omega_a)^2]}{1 - (\omega/\omega_a)^2} \quad (6)$$

where $\Delta\alpha_0^{\text{vis}}(\omega)$ is the contribution from the three transitions at 455, 493, and 614 nm, and $\omega_a = 0.2049(42)$ a.u. is the estimated position of the effective uv pole. This gives $\Delta\alpha_0(0) = -72.60(24)$ a.u., consistent with the theoretical estimate of $-73.1(1.3)$ a.u., although we note that the matrix element $\langle 6P_{3/2} | r | 5D_{5/2} \rangle = 4.0911(31)$ a.u. relies

on a ratio determined from theory.

It should be noted that an alternative value of $\langle 6P_{3/2} | r | 5D_{5/2} \rangle = 4.140(14)$ a.u. can be obtained using the experimental value of $\langle 6P_{3/2} | r | 6S_{1/2} \rangle$ reported in [4], and the $P_{3/2}$ branching ratios reported in [8]. The value is also consistent with the theoretical estimate given in [15] but the theoretical uncertainty in the matrix element is correlated with the uncertainty in the estimated value of ω_0 . Using the alternative experimental value of $\langle 6P_{3/2} | r | 5D_{5/2} \rangle$ in the theory gives a calculated value of $\Delta\alpha_0(\omega_0) \approx 4.5$ a.u and the estimate $\Delta\alpha_0(0) = -76.7(1.2)$ a.u. when applying the formalism in [15] to approximate $\Delta\alpha_0(\omega)$. Both suggest a more significant discrepancy with the estimated uv contributions, which further supports a potential problem with the results in [8] as already noted in [18]. Plans to remeasure the $P_{3/2}$ branching ratios are already in progress.

In summary we have provided an accurate determination of the zero crossing in the dynamic differential scalar polarizability of the $S_{1/2} - D_{5/2}$ clock transition in $^{138}\text{Ba}^+$. Measurements utilized a ratio of scalar to tensor components of the differential polarizability so as to eliminate intensity variations in the Stark-shifting laser. The value of 459.1614(28) THz is in excellent agreement with theory and is a crucial determination for realizing an accurate representation of $\Delta\alpha_0(\omega)$ over a large wavelength range as proposed in [15]. Given the inconsistency of estimated values for $\langle 6P_{3/2} | r | 5D_{5/2} \rangle$, it is desirable to remeasure the $P_{3/2}$ branching ratios as noted in [15, 18] and plans for this are already in progress. With the discrepancy resolved, $\Delta\alpha_0(\omega)$ will be determined with inaccuracies below 0.5% for wavelengths $\gtrsim 700$ nm. This will allow accurate *in situ* calibration of laser intensities, enabling similarly accurate estimates of $\Delta\alpha_0(\omega)$ for other atomic transitions.

ACKNOWLEDGMENTS

This work is supported by the National Research Foundation, Prime Ministers Office, Singapore and the Min-

istry of Education, Singapore under the Research Centres of Excellence programme. M. S. Safronova acknowledges the sponsorship of the Office of Naval Research, USA, Grant No. N00014-17-1-2252.

[1] G Marx, G Tommaseo, and G Werth. Precise g_J - and gr -factor measurements of Ba^+ isotopes. *The European Physical Journal D-Atomic, Molecular, Optical and Plasma Physics*, 4(3):279–284, 1998.

[2] KH Knöll, G Marx, K Hübner, F Schweikert, S Stahl, Ch Weber, and G Werth. Experimental g_J factor in the metastable $5D_{3/2}$ level of Ba^+ . *Physical Review A*, 54(2):1199, 1996.

[3] Matthew R Hoffman, Thomas W Noel, Carolyn Auchter, Anupriya Jayakumar, Spencer R Williams, Boris B Blinov, and EN Fortson. Radio-frequency-spectroscopy measurement of the Landé g_J factor of the $5D_{5/2}$ state of Ba^+ with a single trapped ion. *Physical Review A*, 88(2):025401, 2013.

[4] Shannon L Woods, ME Hanni, SR Lundein, and Erica L Snow. Dipole transition strengths in Ba^+ from rydberg fine-structure measurements in Ba and Ba^+ . *Physical Review A*, 82(1):012506, 2010.

[5] JA Sherman, A Andalkar, W Nagourney, and EN Fortson. Measurement of light shifts at two off-resonant wavelengths in a single trapped Ba^+ ion and the determination of atomic dipole matrix elements. *Physical Review A*, 78(5):052514, 2008.

[6] N Kurz, MR Dietrich, Gang Shu, R Bowler, J Salacka, V Mirgon, and BB Blinov. Measurement of the branching ratio in the $6P_{3/2}$ decay of Ba II with a single trapped ion. *Physical Review A*, 77(6):060501(R), 2008.

[7] D De Munshi, T Dutta, R Rebhi, and M Mukherjee. Precision measurement of branching fractions of $^{138}\text{Ba}^+$: Testing many-body theories below the 1% level. *Physical Review A*, 91(4):040501(R), 2015.

[8] Tarun Dutta, Debashis De Munshi, Dahyun Yum, Riadh Rebhi, and Manas Mukherjee. An exacting transition probability measurement-a direct test of atomic many-body theories. *Scientific reports*, 6:29772, 2016.

[9] C Guet and WR Johnson. Relativistic many-body calculations of transition rates for Ca^+ , Sr^+ , and Ba^+ . *Physical Review A*, 44(3):1531, 1991.

[10] VA Dzuba, VV Flambaum, and JSM Ginges. Calculations of parity-nonconserving $s - d$ amplitudes in Cs , Fr , Ba^+ , and Ra^+ . *Physical Review A*, 63(6):062101, 2001.

[11] E Iskrenova-Tchoukova and MS Safronova. Theoretical study of lifetimes and polarizabilities in Ba^+ . *Physical Review A*, 78(1):012508, 2008.

[12] UI Safronova. Relativistic many-body calculation of energies, lifetimes, hyperfine constants, multipole polarizabilities, and blackbody radiation shift in ^{137}Ba II. *Physical Review A*, 81(5):052506, 2010.

[13] BK Sahoo, BP Das, RK Chaudhuri, and D Mukherjee. Theoretical studies of the $6s\ 2S_{1/2} \rightarrow 5d\ 2D_{3/2}$ parity-nonconserving transition amplitude in Ba^+ and associated properties. *Physical Review A*, 75(3):032507, 2007.

[14] Geetha Gopakumar, Holger Merlitz, Rajat K Chaudhuri, BP Das, Uttam Sinha Mahapatra, and Debashis Mukherjee. Electric dipole and quadrupole transition amplitudes for Ba^+ using the relativistic coupled-cluster method. *Physical Review A*, 66(3):032505, 2002.

[15] MD Barrett, KJ Arnold, and MS Safronova. Polarizability assessments of ion-based optical clocks. *accepted to Phys. Rev. A*, 2019.

[16] Kyle J Arnold, Rattakorn Kaewuam, Arpan Roy, Ting Rei Tan, and Murray D Barrett. Blackbody radiation shift assessment for a lutetium ion clock. *Nature communications*, 9, 2018.

[17] Rattakorn Kaewuam, Arpan Roy, Ting Rei Tan, KJ Arnold, and MD Barrett. Laser spectroscopy of $^{176}\text{Lu}^+$. *Journal of Modern Optics*, 65(5-6):592–601, 2018.

[18] KJ Arnold, SR Chanu, R Kaewuam, TR Tan, L Yeo, Zhiqiang Zhang, MS Safronova, and MD Barrett. Measurements of the branching ratios for $6P_{1/2}$ decays in $^{138}\text{Ba}^+$. *Physical Review A*, 100:032503, 2019.